Onset of intermittency in two-dimensional decaying turbulence

Leslie M. Smith[1] and Victor Yakhot[2]
[1]*Yale University, New Haven, Connecticut 06520*
[2]*Fluid Dynamics Research Center, Princeton University, Princeton, New Jersey 08544*
(Received 4 January 1996; revised manuscript received 26 May 1996)

The statistics of two-dimensional flow decaying from an initially Gaussian velocity field are investigated both theoretically and numerically. During the initial stages of the turbulence decay, small-scale intermittency develops, while the intermediate and large scales remain essentially Gaussian. Corresponding to these early times, an expression describing the evolution of the shape of the probability density $P(\Omega,S_4)$ is derived from the Navier-Stokes equations, where $\Omega=\omega/\omega_{\rm rms}$ is the normalized vorticity and S_4 is the normalized fourth-order moment of the vorticity. Predictions of the theory, which does not involve adjustable parameters, agree with the results of numerical simulations for the early-time decay. [S1063-651X(97)00304-8]

PACS number(s): 47.27.−i

I. INTRODUCTION

Although progress is ongoing, the understanding of intermittency from first principles remains one of the major outstanding problems in turbulence theory. Intermittency in turbulence is evidenced by scale dependence of the normalized even-order moments of the velocity differences [1], where, for example, the longitudinal velocity difference as a function of the displacement scale r is defined by $\Delta u_i(r)\equiv u_i(\mathbf{x}+r\hat{\mathbf{i}})-u_i(\mathbf{x})$. A flow is intermittent if $\langle[\Delta u_i(r)]^{2n}\rangle/\langle[\Delta u_i(r)]^2\rangle^n$ is a function of r. For turbulent flows, the normalized even-order moments increase from the Gaussian values as the displacement r decreases. Intermittency is also manifested in the probability density $P(X)$ by very broad tails for large values of X when X is a derivative-related variable such as the vorticity ω or dissipation-rate fluctuations $\epsilon-\overline{\epsilon}$. It is believed that the tails of $P(X)$ are dominated by coherent structures. However, in three dimensions, little is known about the formation of these structures and their direct effect on the probability densities.

Decaying two-dimensional (2D) turbulence is characterized by the emergence of coherent vortices. A typical numerical experiment deals with the Navier-Stokes equations evolving from an initial condition $\mathbf{v}(\mathbf{k},0)$, usually corresponding to a Gaussian random field with an energy spectrum peaked at some $k=k_0$. It has been convincingly shown that the energy decay in this system is accompanied by the appearance of coherent, long-living vortices that eventually dominate the dynamics of the flow (see, e.g., [2–5]). Since coherent vortices cannot exist in a field which is Gaussian at all scales, their appearance must be accompanied by deviations of the single-point vorticity probability density function (PDF) $P(\Omega,t)$ from the initial Gaussian distribution. Thus, in two dimensions, the formation of coherent vortices is likely to be responsible for the tails of the single-point vorticity PDF $P(\Omega,t)$ and intermittency.

The present investigation provides some quantitative information about the onset of intermittency for the case of 2D decaying turbulence. In this case, there is an extensive literature on the subject of vortex merger and the long-time dynamics (e.g., [6] and [7]). Here the purpose is to investigate the statistical flow properties during the initial stages of the decay from an initially Gaussian velocity field. The present work is thus different from previous studies dealing with much later stages of the evolution of the flow field, when almost the entire vorticity is associated with coherent structures [6] and [7]. Our numerical data show the simultaneous development of small-scale intermittency, as measured by the normalized even-order moments of the velocity differences, and excitations corresponding to the tails of the single-point PDF $P(\Omega,t)$. The (also simultaneous) growth of the maximum of vorticity normalized by the root-mean-square value, reflecting a concentration of vorticity, suggests that the physics underlying the onset of intermittency is indeed the formation of vortices.

In Sec. II we derive the PDF of vorticity in a periodic domain, valid for short times during the decay of 2D turbulence from an initially Gaussian velocity field. In Sec. III we compare the theoretical PDF to the results of high-resolution direct numerical simulations. It will be shown that the theory and the simulations agree for early times, and the later breakdown of the theory is discussed. Moments of the velocity differences measured during the simulations are also presented in Sec. III as a direct measure of intermittency. Section IV describes a simple kinetic model for the growth of intermittency that is motivated by the results of the numerical simulation. This model is used to verify the approximations employed in the derivation of the short-time PDF. The limitations of the theory are further discussed in Sec. IV. A summary is given in Sec. V.

II. THE PROBABILITY DENSITY OF VORTICITY

A. The basic equations

To derive an expression for the single-point vorticity PDF, we apply the formalism developed by Sinai and Yakhot for a passive scalar [8] to the vorticity equation in 2D,

$$\frac{\partial\omega}{\partial t}=-\mathbf{u}\cdot\boldsymbol{\nabla}\omega+\nu\nabla^2\omega, \tag{1}$$

where $\mathbf{u}=u_1(x_1,x_2)\hat{\mathbf{i}}+u_2(x_1,x_2)\hat{\mathbf{j}}$, ν is the molecular viscosity, the vorticity $\omega=\hat{\mathbf{k}}\cdot(\boldsymbol{\nabla}\times\mathbf{u})$ is a pseudoscalar, and $\boldsymbol{\nabla}\cdot\mathbf{u}=0$ for incompressible flow. Multiplying Eq. (1) by ω and aver-

aging over the periodic domain, one finds the expression for the mean dissipation rate of energy $\overline{\epsilon}$,

$$\frac{1}{2}\frac{\partial\overline{\omega^2}}{\partial t}\equiv-\overline{\epsilon}=-\nu\overline{(\nabla\omega)^2}, \tag{2}$$

where the overbar denotes the spatial average, $\overline{\omega^2}\equiv\omega_{\rm rms}^2$, and $(\nabla\omega)^2=\nabla\omega\cdot\nabla\omega$. Introducing the normalized vorticity $\Omega=\omega/\omega_{\rm rms}$ and using Eq. (2), Eq. (1) may be written as

$$-\frac{\Omega}{\omega_{\rm rms}^2}\overline{\epsilon}+\frac{\partial\Omega}{\partial t}=-\mathbf{u}\cdot\nabla\Omega+\nu\nabla^2\Omega. \tag{3}$$

We next multiply Eq. (3) by $2n\Omega^{2n-1}$ to find

$$\begin{aligned}-2n\frac{\Omega^{2n}}{\omega_{\rm rms}^2}\overline{\epsilon}+\frac{\partial\Omega^{2n}}{\partial t}&=-2n\Omega^{2n-1}\mathbf{u}\cdot\nabla\Omega+2n\nu\Omega^{2n-1}\nabla^2\Omega\\&=-\mathbf{u}\cdot\nabla\Omega^{2n}+\nu[\nabla^2\Omega^{2n}\\&\quad-2n(2n-1)\Omega^{2n-2}(\nabla\Omega)^2].\end{aligned} \tag{4}$$

Defining two additional normalized quantities, $y^2\equiv(\nabla\omega)^2/\overline{(\nabla\omega)^2}$ and $dt'\equiv\overline{\epsilon}dt/\overline{\omega^2}$, Eq. (4) may be written as

$$\begin{aligned}-2n\Omega^{2n}+\frac{\partial\Omega^{2n}}{\partial t'}&=-2n(2n-1)\Omega^{2n-2}y^2\\&\quad+\frac{\omega_{\rm rms}^2}{\overline{\epsilon}}[\nu\nabla^2\Omega^{2n}-\mathbf{u}\cdot\nabla\Omega^{2n}].\end{aligned} \tag{5}$$

Averaging Eq. (5) in space, and using the fact that the second and third terms on the right-hand side vanish for periodic boundary conditions (and homogeneous flows), leads to the dynamical equation for the even-order moments $\overline{\Omega^{2n}}$ of the normalized vorticity,

$$-2n\overline{\Omega^{2n}}+\frac{\partial\overline{\Omega^{2n}}}{\partial t'}=-2n(2n-1)\overline{\Omega^{2n-2}y^2}, \tag{6}$$

where $\overline{\Omega^{2n}}=\overline{\omega^{2n}}/(\overline{\omega^2})^n$. The main assumption of the approximation developed herein is that the second term on the left-hand side of Eq. (6) is small compared to the other two terms during the initial stages of the turbulence decay from Gaussian statistics, and this assumption will allow us to derive the short-time PDF of vorticity in closed form without adjustable parameters. Comparison of Eqs. (4) and (6) shows that this assumption can be stated in dimensional terms (inverse time scales) as

$$\left|\frac{1}{\omega_{\rm rms}}\frac{\partial\omega_{\rm rms}}{\partial t}\right|\gg\left|\frac{1}{2n\overline{\Omega^{2n}}}\frac{\partial\overline{\Omega^{2n}}}{\partial t}\right|, \tag{7}$$

which is always true for $n=1$ since $\overline{\Omega^2}=1$ by definition, and can be justified for $n>1$ by a near-Gaussian expansion of the moments of Ω. For a Gaussian field, the odd moments $\overline{\Omega^{2n-1}}$ for $n\geqslant1$ are equal to zero, and the even moments $\overline{\Omega^{2n}}$ for $n\geqslant1$ are constants, for example, the flatness $\overline{\Omega^4}=3$. Therefore it is plausible that $|\partial\overline{\Omega^{2n}}/\partial t'|\ll|2n\overline{\Omega^{2n}}|$ for short times during the decay from Gaussian statistics. The term $\partial\overline{\Omega^{2n}}/\partial t'$ will be carried through several more steps in the analysis for the purpose of deriving its corresponding terms in the equation for the PDF of vorticity.

At this point we introduce the joint PDF $P(\Omega,y,t')=P(\Omega,t')q(y|\Omega,t')$ and assume equivalence between space and ensemble averages such that

$$\overline{\Omega^m}=\int_{-\infty}^{\infty}\Omega^mP(\Omega,t')d\Omega, \tag{8a}$$

$$\begin{aligned}\overline{\Omega^my^2}&=\int_{-\infty}^{\infty}\int_{-\infty}^{\infty}\Omega^my^2P(\Omega,y,t')d\Omega\ dy\\&=\int_{-\infty}^{\infty}\Omega^mP(\Omega,t')q_0(\Omega,t')d\Omega,\end{aligned} \tag{8b}$$

where $q_0(\Omega,t')$ is the conditional expectation value of y^2 for given Ω,

$$q_0(\Omega,t')=\int_{-\infty}^{\infty}y^2q(y|\Omega,t')dy. \tag{9}$$

In addition, we have the normalization relations

$$\begin{aligned}\int_{-\infty}^{\infty}\Omega^2P(\Omega,t')d\Omega&=\int_{-\infty}^{\infty}q_0(\Omega,t')P(\Omega,t')d\Omega\\&=\int_{-\infty}^{\infty}P(\Omega,t')d\Omega=1,\end{aligned} \tag{10}$$

where the first and second conditions follow from the definitions $\Omega\equiv\omega/\omega_{\rm rms}$ and $y^2=(\nabla\omega)^2/\overline{(\nabla\omega)^2}$, respectively, and the third condition follows from the definition of the PDF $P(\Omega,t')$. From the assumption of equivalence between space and ensemble averaging (8a), (8b), Eq. (6) may be written in terms of $P(\Omega,y,t')$ as

$$\begin{aligned}-2n\int_{-\infty}^{\infty}\Omega^{2n}P(\Omega,t')d\Omega+\int_{-\infty}^{\infty}\Omega^{2n}\frac{\partial P(\Omega,t')}{\partial t'}d\Omega\\=-2n(2n-1)\int_{-\infty}^{\infty}\Omega^{2n-2}P(\Omega,t')q_0(\Omega,t')d\Omega.\end{aligned} \tag{11}$$

Using the boundary conditions $P(\Omega,t')\to0$ for $\Omega\to\pm\infty$, one integration by parts of the first term on the left-hand side of Eq. (11), and two integrations by parts of the term on the right-hand side of Eq. (11), lead to

$$\begin{aligned}\int_{-\infty}^{\infty}\Omega^{2n}\frac{\partial\Omega P(\Omega,t')}{\partial\Omega}d\Omega+\int_{-\infty}^{\infty}\Omega^{2n}\frac{\partial P(\Omega,t')}{\partial t'}d\Omega\\=-\int_{-\infty}^{\infty}\Omega^{2n}\frac{\partial^2P(\Omega,t')q_0(\Omega,t')}{\partial\Omega^2}d\Omega.\end{aligned} \tag{12}$$

Since Eq. (12) should hold for any value of n, it is reasonable to conclude that

$$\frac{\partial\Omega P(\Omega,t')}{\partial\Omega}+\frac{\partial P(\Omega,t')}{\partial t'}=-\frac{\partial^2P(\Omega,t')q_0(\Omega,t')}{\partial\Omega^2}. \tag{13}$$

Equation (13) describes the evolution of $P(\Omega,t')$ in a periodic domain, where the only assumption, thus far, is the equivalence of space and ensemble averaging.

B. The short-time approximation

At this point we make the definitive assumption of the theory, namely, that the explicit time-derivative term on the left-hand side of Eq. (13) is negligible for short times, leading to

$$\frac{\partial\Omega P(\Omega,t')}{\partial\Omega}=-\frac{\partial^2 P(\Omega,t')q_0(\Omega,t')}{\partial\Omega^2}. \tag{14}$$

Direct integration then yields the short-time solution [8]

$$P(\Omega,t')=\frac{C(t')}{q_0(\Omega,t')}\exp\left[-\int_0^\Omega\frac{u\,du}{q_0(u,t')}\right], \tag{15}$$

where $P(\Omega,t')$ is a functional of $q_0(\Omega,t')$. Notice that Eq. (15) follows directly from Eq. (6) neglecting the term $\partial\overline{\Omega^{2n}}/\partial t'$. In Sec. III we provide a consistency check of the short-time solution (15) by verifying the relation

$$\left|\frac{\partial P(\Omega,t')}{\partial t'}\right|\ll\left|\frac{\partial\Omega P(\Omega,t')}{\partial\Omega}\right| \tag{16}$$

for early times during the numerical simulation.

To understand the short-time PDF (15), recall that $q_0(\Omega,t')$ is the conditional value of $y^2=(\nabla\omega)^2/\overline{(\nabla\omega)^2}$ for a given value of Ω. If $q_0(\Omega,t')\approx A$ constant, then Eq. (15) has the Gaussian form given by $P(\Omega,t')\approx(C/A)\exp(-\Omega^2/2A)$, where $C=(A/2\pi)^{1/2}$. The normalization constraints (10) require that A must be equal to unity, and thus we obtain the asymptotic result $q_0(\Omega,t')\approx A=1$ for $t'\to 0$. Since by isotropy $q_0(\Omega,t')=q_0(-\Omega,t')$, and assuming analysticity of $q_0(\Omega,t')$, one may write

$$q_0(\Omega,t')=A(t')+\sum_{n=1}^{\infty}B_{2n}(t')\Omega^{2n}, \tag{17a}$$

where $A\to 1$ and $B_{2n}\to 0$ for small times t' during the decay from an initially Gaussian field. As the flow field decays, the tails of the PDF deviate from the Gaussian solution to include larger values of Ω (see Fig. 2). At first, the term $B(t')\Omega^2$ is likely to contribute the largest correction to the Gaussian solution. Neglecting terms for $n\geqslant 2$ and dropping the subscript from B_2, we expect

$$q_0(\Omega,t')\sim A(t')+B(t')\Omega^2, \tag{17b}$$

for $t'\to 0$.

Before proceeding to find the coefficients A and B of the series expansion for $q_0(\Omega,t')$, we would like to summarize the previous analysis and to reiterate the physical content of the short-time solution (15). Rewriting Eq. (1) in terms of the normalized vorticity $\Omega=\omega/\omega_{\rm rms}$ we have assumed that the time scale $\omega_{\rm rms}(d\omega_{\rm rms}/dt)^{-1}$ is much smaller than the time scale $2n\overline{\Omega^{2n}}(\partial\overline{\Omega^{2n}}/\partial t)^{-1}$, which is a near-Gaussian approximation and constitutes the main assumption of the theory. Introducing $\overline{\epsilon}=-\omega_{\rm rms}d\omega_{\rm rms}/dt$ and the normalized time differential $dt'=\overline{\epsilon}dt/\overline{\omega^2}$ leads ultimately to the solution (15) with time dependence entering implicitly through $q_0(\Omega,t')$. The quantity $q_0(\Omega,t')$ is governed by an evolution equation that may be derived from the equation for $\nabla\omega$ by a sequence of steps similar to those above. Since the advective nonlinearity in the vorticity equation (1) will generate a term representing the stretching of $\nabla\omega$ that will not vanish upon spatial integration over the periodic domain, nonlinear effects also enter Eq. (15) implicitly through $q_0(\Omega,t')$. Thus time dependence and nonlinearity both enter Eq. (15) through the higher-order terms in the series expansion (17a) for $q_0(\Omega,t')$. Linear theory corresponds to the Gaussian solution following from $q_0(\Omega,t')\approx A=1$. We will now find the probability density $P(\Omega,t')$ including time dependence and nonlinear effects by retaining the term $B(t')\Omega^2$ in the expansion (17).

C. The series expansion for $q_0(\Omega,t')$

The dynamical equation for $q_0(\Omega,t')$ contains the full nonlinearity and time dependence of $q_0(\Omega,t')$. However, here we will use instead: (i) the series expansion (17) truncated at $B(t')\Omega^2$, valid for short times; (ii) the dynamical equation (6) for $\overline{\Omega^{2n}}$ neglecting $\partial\overline{\Omega^{2n}}/\partial t'$ for consistency with Eq. (15); (iii) the three normalization constraints (10). As will be shown, these are sufficient to specify the short-time PDF (15) in closed form without adjustable parameters.

To describe the numerical simulations, we use a nondimensional time T defined by $T\equiv\int_0^t d\tau\, u_{\rm rms}(\tau)k_p(\tau)/\pi$, where $u_{\rm rms}(t)$ is the root-mean-square velocity, $k_p(t)$ is the wave number of the peak of the energy spectrum, the normalization factor π is the largest independent length scale in the system and $[u_{\rm rms}(\tau)k_p(\tau)/\pi]^{-1}$ is an approximate eddy turnover time associated with $u_{\rm rms}$. As will be discussed in Secs. III and IV, the numerical data show that there exists a characteristic time scale $T=T_c$ such that the statistics of the velocity field are close to Gaussian for $T<T_c$, with deviations from the Gaussian values building up for $T>T_c$. Thus we make the equivalence between $t'\to 0$ and $T\to T_c^+$ for the comparison between the theory and the numerical simulations.

As noted above, $q_0(\Omega,T)\approx A=1$ for $T<T_c$. At larger times $T>T_c$, the tails $|\Omega|\gg 0$ of the PDF $P(\Omega,T)$ grow and, according to Eq. (17b), one may write $q_0(\Omega,T)\approx A(T)+B(T)\Omega^2$ with $A(T)\to 1$ and $B(T)\to 0$ for $T\to T_c^+$. Using the normalization constraints (10), one finds

$$A(T)=1-B(T). \tag{18}$$

The function $B(T)$ may be found from the dynamical equation (6) for Ω^{2n}. Introducing the notation $S_{2n}\equiv\overline{\Omega^{2n}}$, using Eqs. (17b) and (18) for $q_0(\Omega,t')$, and neglecting $\partial\overline{\Omega^{2n}}/\partial t'$ for consistency with the PDF (15), one finds from Eq. (6) the recursion relation

$$S_{2n}=(2n-1)(1-B)S_{2n-2}+(2n-1)BS_{2n}. \tag{19}$$

Setting $n=2$ and using the normalization constraint $S_2=1$ [the first constraint (10)] then leads to

$$B=\frac{1}{(S_4-1)}\frac{(S_4-3)}{3}, \tag{20}$$

which has the required behavior $B(T)\to 0$ as $T-T_c\to 0$ since $S_4-3\to 0$ for $T-T_c\to 0$. The short-time recursion relation (19) says that the higher-order moments S_{2n} for $n\geqslant 3$ can be expressed in terms of the flatness S_4 only. Substituting Eq. (17b) for $q_0(\Omega,t)$ into the PDF (15) gives

$$P(\Omega,S_4)=C(B)(A(B)+B(S_4)\Omega^2)^{-[1+1/2B(S_4)]}, \quad (21)$$

where the parameter $C(B)$ is found from the third normalization constraint (10). The coefficients of the theory $A(B)$, $B(S_4)$ and $C(B)$ are given self-consistently by Eq. (6) and the constraints (10), and thus the PDF (21) satisfies the definition $S_4=\int_{-\infty}^{\infty}P(\Omega,S_4)\Omega^4 d\Omega$. The short-time solution (21) for the PDF describes the shape of the vorticity probability density $P(\Omega,S_4)$ in 2D turbulence decaying from an initially Gaussian velocity field in a periodic domain. The limits of validity of Eq. (21) will be discussed below in detail.

Owing to the near-Gaussian approximation (7) leading to Eq. (21), the explicit time dependence of the coefficients is not given by the theory. However, the time evolution of one coefficient determines the time evolution of the remaining four coefficients and therefore the PDF itself. In Sec. III we compare theory and experiment as a function of S_4, where, as in Eq. (21), the time dependence is implicit in S_4. Based on the numerical simulation data, a model evolution equation for $S_4(T)$ is proposed in Sec. IV to provide a formula for the explicit time dependence of $P(\Omega,T)$. The purpose of this model is to justify the main assumption of the theory by verifying the relation (16) for short times $T-T_c^+\to 0$ during the numerical simulation.

III. COMPARISON TO THE RESULTS OF DIRECT NUMERICAL SIMULATION

To test the theoretical predictions given above, we have conducted numerical experiments of decaying 2D turbulence. The equation of motion (1) was written in terms of a stream function ψ

$$\frac{\partial\omega}{\partial t}-\frac{\partial\psi}{\partial x_1}\frac{\partial\omega}{\partial x_2}+\frac{\partial\psi}{\partial x_2}\frac{\partial\omega}{\partial x_1}=\nu\nabla^2\omega, \quad (22)$$

where $\omega=-\nabla^2\psi$ with $u_1=\partial\psi/\partial x_2$ and $u_2=-\partial\psi/\partial x_1$. A pseudospectral code was used to solve Eq. (22) in a periodic square at resolutions $\mathcal{N}=512^2$ and 1024^2. As initial condition in each run, we took a stream function $\psi_0(\mathbf{k})$ with independent Gaussian real and imaginary parts and a velocity spectrum $E_0(k)$ peaked about k_0: $E_0(k)=Ae^{-10(k-k_0)^2}$ with ratios $k_0/\mathcal{N}$ varying from 0.2 to 0.05. The energy spectrum $E(k)$ is given in terms of $\psi(k)$ by the relation $E(k)=\pi k^3\langle\psi(\mathbf{k})\psi(-\mathbf{k})\rangle$, where the brackets indicate an average over angles. In all cases, we found that deviations from Gaussian statistics appeared at time $T=T_c\approx 5$ independent of the value of $k_0/\mathcal{N}$. Apparently, the nondimensional time scale T is approximately the correct rescaling of time for a theory of the single-point PDF independent of the initial values of energy, entropy and Reynolds number. The time T_c is the time for population of modes up to the dissipation wave number k_d owing to nonlinear interactions.

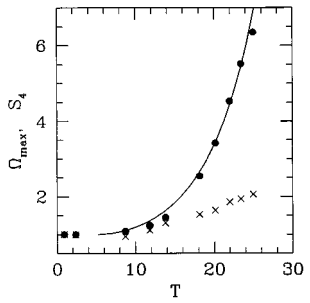

FIG. 1. $\Omega_{\max}(T)/\Omega_{\max}(T=0)$ (crosses); $S_4(T)/3$ (solid circles). The line is formula (25) with $\alpha=0.18$ and $\beta=0.09$.

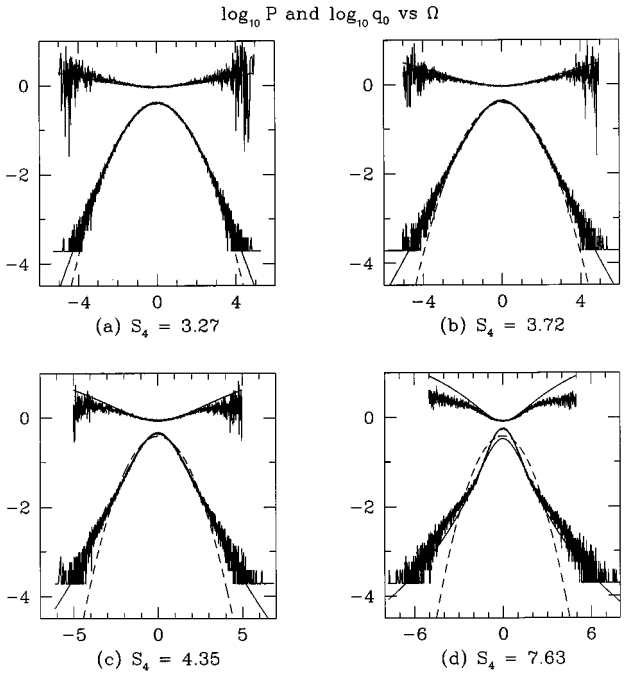

FIG. 2. $\log_{10} q_0(\Omega)$ and $\log_{10} P(\Omega)$ vs Ω at (a) $S_4=3.27$ ($T=8.7$), (b) $S_4=3.72$ ($T=11.8$), (c) $S_4=4.35$ ($T=13.8$), and (d) $S_4=7.63$ ($T=18.2$). The solid lines are the theoretical predictions for $q_0(\Omega)$ (17b), (18), and (20) and $P(\Omega)$ (21) for the same S_4 as the experimental PDF, and the dashed line is the Gaussian distribution.

Here we present the results for $\mathcal{N}=1024$, $k_0=100$, and $A=0.01$. We used a variable viscosity $\nu(t)=\mu\omega_{\rm rms}(t)/k_{\max}^2$ following [9], where $\omega_{\rm rms}(t)$ is the root-mean-square vorticity, $k_{\max}=1024/3$ is the dealiasing wave number, and $\mu=0.2$ is a constant. This avoids temporary resolution problems due to the high total entropy initially present in the flow. As one indicator of coherence, we measured the single-point vorticity flatness S_4. The time evolution of S_4 is presented in Fig. 1 (dark circles), which shows that S_4 departs from the Gaussian value of three at a time $T=T_c\approx 5$. Figure 2 shows the single-point vorticity probability distribution $P(\Omega,S_4(T))$ as well as the conditional expectation $q_0(\Omega,S_4(T))$ at four values of S_4 (increasing times) after the onset of intermittency. The probability density $P(\Omega,T)$ was obtained from the experimental data by counting the points $N(\Omega)$ in the vorticity field corresponding to the value of Ω in the interval $(\Omega,\Omega+\delta\Omega)$. In this way $P(\Omega,T)=N(\Omega)/N$. Similarly, for a given value $\Omega=\Omega_1$ in the interval $(\Omega_1,\Omega_1+\delta\Omega)$, $q_0(\Omega_1,T)=\Sigma\, y^2/N(\Omega_1)$ is the sum of the values of y^2 at each grid point where $\Omega=\Omega_1$, divided by the

TABLE I. Maximum and average values of F_{2n}, $n=2-4$; $\Omega_{\max}$; S_4.

T	$\overline{r}$	max F_4	avg F_4	max F_6	avg F_6	max F_8	avg F_8	$\Omega_{\max}$	S_4
8.7	0.086	3.16	3.04	17.59	15.74	144.09	116.19	5.30	3.27
11.8	0.200	3.11	3.04	16.74	15.71	131.80	115.30	6.19	3.72
13.8	0.012	3.11	3.02	17.06	15.32	138.88	110.02	7.28	4.35
18.2	0.012	3.36	3.04	21.48	15.69	217.53	115.7	8.56	7.63
25.0	0.012	4.26	3.16	46.18	17.72	775.72	151.72	15.33	19.05

total number of points with $\Omega=\Omega_1$. The interval $-\Omega_{\max}<\Omega<\Omega_{\max}$ was subdivided into approximately 2000 bins (the number of bins increased as $\Omega_{\max}$ increased).

We have analyzed the moments of vorticity S_{2n} up to eighth order and found that for the short times [Figs. 2(a) and 2(b)], the agreement between theory and experiment is excellent. Somewhat later when $S_4\approx 4.3$ [Fig. 2(c)], the tails of the experimental $q_0(\Omega,T)$ can be seen to depart from the theoretical $q_0(\Omega,T)$, and the departure increases as time increases and S_4 grows large compared to the Gaussian value [Fig. 2(d)]. The discrepancy between the theoretical PDF (21) and the experimental PDF is expected to grow at the larger times of our simulation.

In a finite system, there is the inevitable lack of a suitable ensemble and uncertainty of the experimental determination of $P(\Omega,T)$) when Ω is large. Thus it is expected that in higher-resolution systems, the quality of prediction will improve even at some what longer times. However, the final state ($T\to\infty$) of decaying 2D turbulence consists of a small number of vortices, and thus the PDF description of the flow based on perturbation from an initial Gaussian state inevitably becomes invalid. Even at short times the expression (21) for the PDF is valid only when Ω is not too large since $\overline{\Omega^{2n}}<\infty$ was assumed in the derivation of Eq. (21). This means that for $\Omega\to\infty$, $P(\Omega,T)$ must tend to zero much faster than predicted by Eq. (21).

In addition to the PDF of vorticity, we also calculated the normalized even-order moments of the longitudinal velocity differences $F_{2n}(r)=\langle[\Delta u_i(r)]^{2n}\rangle/\langle[\Delta u_i(r)]^2\rangle^n$, $n=1-4$, averaged over space. Table I gives the maximum and average values of $F_{2n}(r)$ for $n=2-4$ at the same four times $T=8.7$, 11.8, 13.8, and 18.2 after the onset of intermittency as in Fig. 2; Fig. 3 shows the full r dependence of $F_8(r)$ at these times. [The behaviors of $F_4(r)$ and $F_6(r)$ are qualitatively similar to that of $F_8(r)$, but the evolution of $F_8(r)$ was chosen for presentation because the growth rate of $F_8(r_{\min})$ is the largest.] For reference, recall that the Gaussian values are $F_4=3$, $F_6=15$, and $F_8=105$. Defining the displacement r corresponding to the maximum value of $F_8(r)$ to be $\overline{r}$, one sees that, for the two earlier times $T=8.7$ and $T=11.8$, the $\overline{r}$ is small but larger than the smallest measured value $r_{\min}=2\pi/512\approx 0.012$ corresponding to two grid points. The global maximum of F_8 occurring at $\overline{r}$ reflects clumping of vorticity on the order of this small length scale $0.012=r_{\min}<\overline{r}\ll r_{\max}=\pi$. At the two later times $T=13.8$ and $T=18.2$, the presence of small-scale intermittency is clearly indicated by a sharp increase of the moments at the smallest measured scales $r_{\min}=0.012$ [see Figs. 3(c), 3(d), and Table I]. Although the presence of other relative maxima shows that clumping at larger scales may be occurring, the dominant concentration of vorticity is evidently at the smallest scales.

The values of the moments $F_{2n}(r_{\min})$ at the smallest measured scale $r_{\min}$ are seen to increase continuously in time until for $T>12$, $F_{2n}(r_{\min})$ is the maximum value of $F_{2n}(r)$ over the entire range of $r_{\min}<r<r_{\max}$. After time $T=12$, the moments settle down to the Gaussian value at intermediate and large scales r, showing that there is only *small-scale* intermittency in the system. By the time $T=18.2$, the peak values at $r_{\min}$ are significantly larger than Gaussian and the intermittency is developed, while we can describe the previous times $5<T<14$ as the period of the onset of intermittency. Table I and Fig. 1 show that this onset is accompanied simultaneously by the growth of $\Omega_{\max}$ and S_4 away from their initial values. Although vortices are not yet developed enough for clear visualization, the growth of $\Omega_{\max}$ suggests their ensuing presence. In other words, the *onset* of coherence is best detected by the statistics. The growth of $\Omega_{\max}$ is also seen in Fig. 2, where for all times there exists an extreme value $\Omega_{\max}$ such that $P(\Omega,T)=0$ for $|\Omega|>\Omega_{\max}$. The magnitudes of both $\Omega_{\max}$ and $P(\Omega_{\max})$ grow with time, suggesting a strengthening of the small-scale vorticity patches as well as an increase in their number.

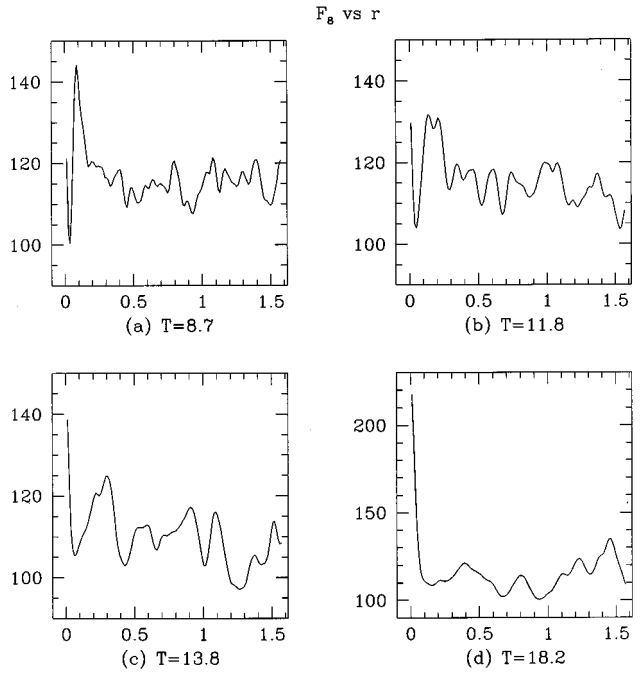

FIG. 3. $F_8(r)$ at the same times as in Fig. 2: (a) $T=8.7$, (b) $T=11.8$, (c) $T=13.8$, and (d) $T=18.2$.

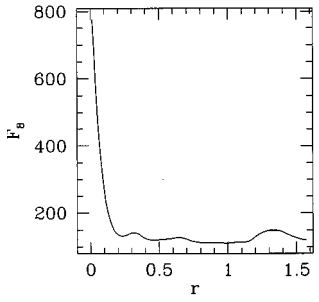

FIG. 4. $F_8(r)$ at $T=25$.

Finally, Fig. 4 shows $F_8(r)$ at $T=25.0$ to illustrate the signature of the flow after intermittency is well developed. At this late time, vorticity is highly concentrated at the smallest scales and clumping at other scales is negligible. By comparison to Fig. 3(d), one sees that the width of the small-scale structures is growing as well as their strength, reflecting the attraction and consumption by the emerging vortices of like-signed vorticity from the background field.

IV. A MODEL FOR THE GROWTH OF INTERMITTENCY

In this section we present a model for the growth of $S_4(T)$ based on the results of our numerical simulations and the suggested link between the onset of intermittency and the generation of coherent vortices. The purpose of this model is to check relation (16) that constitutes the main assumption of the theory presented in Sec. II. According to Figs. 1 and 2, the early stages of the dynamics of coherent-structure generation can be characterized by two distinct regimes. First, at $T\approx T_c$, the nonlinear interaction between the modes of an initially Gaussian velocity field leads to the formation of weak patches of vorticity responsible for small deviations from Gaussian statistics. The second stage can be described by the following simple model: the strongest emerging vorticity patches, corresponding to the tails of the distribution function $P(\Omega,T)$, grow by subsuming the surrounding weak excitations having vorticity of the same sign. This is consistent with the negative sign of the effective viscosity in 2D turbulence [10] and for 2D arrays of vortices [11]. If we denote the typical vorticity of these patches as $\Omega_0(T)$, then the rate of depletion of the random background field increases with increasing $\Omega_0(T)$. The growth of $\Omega_0(T)$ in the strengthening vortices is given by the differential equation

$$\frac{d\Omega_0(T)}{dT}\approx\frac{\Omega_0(T)}{\tau_0(T)}, \tag{23}$$

where all variables are nondimensional, and the characteristic time scale $\tau_0(T)$ is inversely proportional to the effective diffusivity $\kappa(T)$ of the background field at the scale of the emerging vortices, $\tau_0(T)\propto 1/\kappa(T)$. Assuming the exponential form $\exp(-\beta t)$ for the time correlation of the velocity leads to

$$\kappa(T)\propto\int_0^T\langle v(t')v(0)\rangle dt'\propto 1-\exp(-\beta T) \tag{24}$$

where the parameter β reflects the time-lagging effect due to the finite time required for vortex generation.

During the second stage of the early-time dynamics, we assume that the deviations from Gaussian statistics are proportional to the typical vorticity $\Omega_0(T)$ of the emerging vortices, e.g., $S_4(T)\propto\Omega_0(T)$. From this assumption and Eqs. (23) and (24), one finds

$$S_4(T-T_c)=3.0\,\exp\left[\alpha\left(T-T_c-\frac{1-\exp[-\beta(T-T_c)]}{\beta}\right)\right],\qquad T>T_c \tag{25}$$

where $T_c\approx 5$ is a parameter of the problem. Figure 1 compares the model solution (25) with the results of the numerical simulation for the values of the constants $\alpha=0.18$ and $\beta=0.09$. Figure 1 shows that it is indeed the case that $S_4(T)\propto\Omega_{\max}$ for $T<15$ corresponding to Figs. 2(a)–(c). Since $\Omega_{\max}$ is the vorticity of the strongest growing vortices, the short-time PDF (21) and the model (25) for $S_4(T-T_c)$ establish a direct dynamic link between the emergence of coherent structures and the shape of probability density $P(\Omega,T)$ in decaying 2D turbulence.

Using the kinetic model (25), $q_0(\Omega,T)$ given by Eqs. (17b), (18), and (20), and $P(\Omega,T)$ given by Eq. (21), one may check the inequality (16). It is straightforward to calculate that

$$\frac{\partial\Omega P(\Omega,T)}{\partial\Omega}=-\frac{\partial^2 P(\Omega,T)q_0(\Omega,T)}{\partial\Omega^2}=O(P(\Omega,T)). \tag{26}$$

Then since the coefficients A and C depend on B, and the coefficient B depends on S_4, one finds

$$\frac{\partial P(\Omega,T)}{\partial T}=\frac{\partial P(\Omega,T)}{\partial B}\frac{\partial B}{\partial S_4}\frac{\partial S_4}{\partial T}=O((T-T_c)P(\Omega,T)). \tag{27}$$

Relations (26) and (27) thus verify relation (16) for $T\to T_c^+(t'\to 0)$. However, the approximation (21) cannot be valid for the evaluation of S_{2n} when $n\to\infty$ even at short times. To illustrate, we rewrite the recursion relation (19) as

$$S_{2n}(T)=(2n-1)S_{2n-2}(T)\frac{1-B(T)}{1-(2n-1)B(T)}. \tag{28}$$

Since $S_{2n}(T)\equiv\overline{\Omega^{2n}}>0$, relation (28) cannot be correct for an arbitrarily large n, even at short times, when $B(T)$ is small but finite. Thus the results of this work are applicable only to low-order moments. This restriction is a direct consequence of the short-time approximation of neglecting the time-derivative term in Eq. (6) together with truncation of the series expansion (17a).

V. SUMMARY

We have shown that the dynamical processes reflected in Figs. 1–4 are best described by two stages. During the first period $0<T<T_c$, the nonlinear interaction populates modes up to the dissipation wave number k_d, but the initially Gaussian velocity field is not substantially distorted. During

the second stage for $T-T_c$ not too large, the even-order moments of the velocity differences show that small-scale intermittency develops, and the tails $|\Omega| \gg 0$ of the PDF $P(\Omega,T)$ grow and change shape. The increasing value of $\Omega_{\max}(t)$ provides a connection between the onset of intermittency during the second stage and the emergence of coherent vortices. A self-acceleration process is suggested, whereby larger amplitude vorticity blobs corresponding to the tails of the vorticity PDF begin to dominate the flow: these weakly interacting patches of vorticity attract and subsume nearby, like-signed vorticity. They ultimately form coherent structures, and will influence each other and eventually merge only at much later times not reached in our simulations (see [2–7]). At these later times we expect the typical vorticity Ω_0 of the vortices and the moments of the vorticity to grow at a rate slower than exponential.

Consistent with this picture, we have derived the single-point vorticity PDF valid for short times during the decay of 2D turbulence away from an initially Gaussian velocity field. The theory can be described as weakly nonlinear and results in the PDF $P(\Omega,S_4)$ as a function of the normalized fourth-order moment S_4 of the vorticity. All coefficients of the theory are determined self-consistently with $S_4 = \int_{-\infty}^{\infty} P(\Omega,S_4)\Omega^4 d\Omega$. Theory and simulations agree for small departures of S_4 from the Gaussian value $S_4=3$ corresponding to short times $T-T_c \to 0$. Together the theory and simulations establish a link between the development of coherent vortices as measured by the growth of $\Omega_{\max}$, and the onset of small-scale intermittency as measured both by the moments of the velocity differences and by the shape of the tails of the vorticity PDF.

ACKNOWLEDGMENTS

The authors gratefully acknowledge the support of ONR through Contract Nos. ONR N00014-94-1-0124 (L. Smith) and ONR N00014-92-J-1363 (V. Yakhot). Eric Jackson has contributed to this work through many valuable suggestions. L. Smith would also like to thank Fabian Waleffe, Ira Bernstein, and Katepalli Sreenivasan for helpful discussions. The computations were performed on the 32-processor IBM PVS parallel computer at Princeton University.

[1] K. R. Sreenivasan, in *Proceedings of the Twelfth Australian Fluid Mechanics Conference*, edited by R. W. Bilger (University of Sydney, Sydney, Australia, 1995), pp. 549–556.
[2] J. C. McWilliams, J. Fluid Mech. **146**, 21 (1984).
[3] A. Babiano, C. Basdevant, B. Legras, and R. Sadourny, J. Fluid Mech. **183**, 379 (1987).
[4] P. Santangelo, R. Benzi, and B. Legras, Phys. Fluids A **1**, 1027 (1989).
[5] D. G. Dritschel, Phys. Fluids A **5**, 984 (1993).
[6] G. F. Carnevale, J. C. McWilliams, Y. Pomeau, J. B. Weiss, and W. R. Young, Phys. Fluids A **4**, 1314 (1992).
[7] J. B. Weiss and J. C. McWilliams, Phys. Fluids A **5**, 608 (1993).
[8] Y. G. Sinai and V. Yakhot, Phys. Rev. Lett. **63**, 1962 (1989).
[9] M. E. Maltrud and G. K. Vallis, J. Fluid Mech. **228**, 321 (1991).
[10] R. H. Kraichnan, J. Atmos. Sci. **33**, 1521 (1976).
[11] G. Sivashinsky and V. Yakhot, Phys. Fluids **28**, 1040 (1985).